16. J. H. Yoo, O. V. Borisov, X. Mao, and R. E. Russo, "Existence of phase explosion during laser ablation and its effects on inductively coupled plasma-mass spectroscopy," Anal. Chem. **73**(10), 2288–2293 (2001).
17. C. Phipps, *Laser Ablation and its Applications* (Springer, 2007).

1. Introduction

Optical coherence tomography (OCT) has proven to be a valuable tool based on low-coherence interferometry for micrometer-scale tomographic imaging of turbid media in a diverse range of applications [1,2]. In OCT, the ability to acquire images at high speeds is strongly desirable for a few practical reasons. First, high-speed OCT is useful for probing rapid dynamics and immune to motion artifacts caused by the moving sample or environment in biomedical settings [2–8]. Second, for industrial applications, fast image acquisition is required for inspecting a large quantity of pieces in a short period of time as well as for imaging a large field of view [9–11]. For these reasons, the frequency-domain OCT methods are preferred for field use as they provide higher scan rates and signal-to-noise ratio than the traditional time-domain method [2–8].

In the last decade, efforts have been made for faster OCT. First, a high-speed frequency-sweeping technique known as Fourier-domain mode locking (FDML) has been developed through pioneering work of Huber *et al* [3,4] to perform swept-source OCT at MHz axial scan rates. Different from the operation of conventional frequency-swept lasers, FDML drives an intra-cavity tunable band-pass filter at a period matched with the round-trip time of the cavity and hence overcomes the trade-off between the laser linewidth (i.e., axial range) and build-up time (i.e., sweep rate), producing axial scan rates as high as 5.2 MHz [4]. Another technique that achieves MHz axial scan rates is Fourier-domain OCT with optical demultiplexers recently developed by Choi *et al* [5]. This method replaces the slow spectrometer with a pair of optical demultiplexers and photodiode arrays, leading to an impressive axial scan rate of 60 MHz at 1560 nm [5]. Finally, the spectrum-stretching method known as frequency-to-time mapping [6,7], dispersive Fourier transformation [12,13], or photonic time-stretch [14,15] has also been shown to provide MHz axial scan rates. This method maps the spectrum of an optical pulse into a temporal waveform using a dispersive element (e.g., a dispersive fiber or chirped fiber Bragg grating) with large group-velocity dispersion (GVD). The resultant chirped pulse train behaves as a passive frequency-swept source, enabling OCT at the axial scan rate equivalent to the pulse repetition rate of the laser [6,7,12–15]. Unfortunately, while photonic time-stretch is effective for ultrafast OCT, its application has, until now, been limited to the fiber-optic communication band (~1550 nm) [6,7,12–15] due to the lack of dispersive elements in the non-telecommunication band, restricting its practical utility.

In this paper, we present high-throughput OCT based on photonic time-stretch in the 800 nm spectral range that offers an axial scan rate of more than 90 MHz – three orders of magnitude higher than conventional OCT in this spectral range. This is made possible by employing a single-mode fiber with a smaller effective mode area (4 μm mode field diameter) than conventional fibers in the wavelength operation range (typically 5 – 6 μm mode field diameter). The fiber, hence, provides increased contribution of waveguide dispersion to the total chromatic dispersion of the fiber, enabling photonic time-stretch. As opposed to the 1550 nm spectral range where water absorption is strong, the 800 nm band is useful for OCT's broad range of applications since its axial resolution improves with shorter wavelengths for a fixed optical bandwidth. As a proof-of-principle demonstration, we show a record high axial scan rate of 90.9 MHz. Furthermore, to show the potential utility of our method, we perform real-time monitoring of laser ablation dynamics. Our method is expected to be useful for industrial applications where the speed of conventional OCT falls short, such as material characterization, microfluidics, and manufacturing and process control.

#166938 - $15.00 USD Received 18 Apr 2012; revised 20 Jun 2012; accepted 22 Jun 2012; published 13 Aug 2012

2. High-throughput OCT

2.1 Schematic

The optical layout for our high-throughput OCT, which we refer to as time-stretch OCT, is schematically shown in Fig. 1. The optical source is a mode-locked Ti:Sapphire femtosecond pulse laser that generates a broadband pulse train at a pulse repetition rate of 90.9 MHz. The light is filtered by a band-pass filter, resulting in a center wavelength and bandwidth of 815 nm and 14 nm, respectively, and then enters the photonic time stretcher that consists of a prism-based pre-chirper and dispersive fiber. The pre-chirper is necessary to avoid unwanted supercontinuum generation in the dispersive fiber. The spectrum of each broadband pulse is converted into a temporal waveform by the large GVD of the dispersive fiber (–615 ps/nm), and then each frequency component of the spectrum illuminates the sample successively in time. The back-reflected pulses from different layers of the sample are interferometrically combined with a reference pulse at the beamsplitter, resulting in an interference fringe in the time domain where the axial information of the sample is encoded. The returned pulse is directed via the optical circulator toward the high-speed amplified photodetector with 12 GHz bandwidth and is digitized by the real-time digitizer with 16 GHz bandwidth and 50 GS/s sampling rate. Inverse Fourier transformation is performed digitally on each measured pulse to obtain the axial profile of the sample. For tomographic image acquisition, an acousto-optic deflector (AOD) is used for high-speed lateral scanning over the sample with 132 resolvable points at 50 kHz.

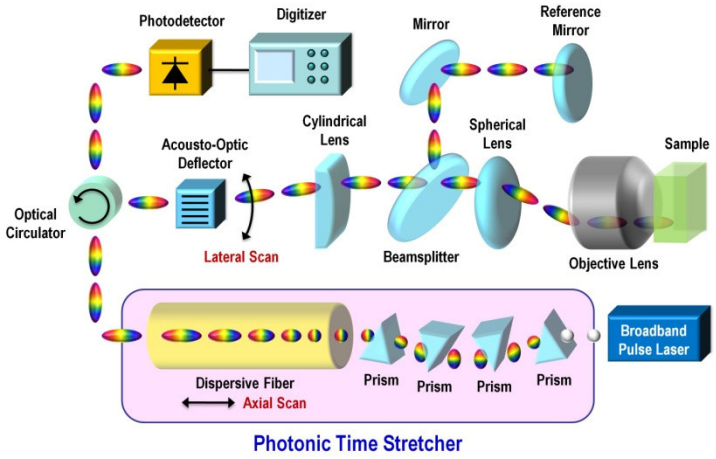

Fig. 1. Schematic of time-stretch OCT. The optical source is a mode-locked Ti:Sapphire femtosecond pulse laser that generates a broadband pulse train at a repetition rate of 90.9 MHz. The photonic time stretcher that consists of a prism-based pre-chirper and dispersive fiber maps the spectrum of each pulse into a temporal waveform which is incident onto the sample. Here each frequency component of the spectrum illuminates the sample successively in time. The back-reflected pulses from different layers of the sample are interferometrically combined with a reference pulse at the beamsplitter, resulting in an interference fringe in the time domain where the axial information of the sample is encoded. The returned pulse is directed via the optical circulator toward the high-speed photodetector and is digitized by the real-time digitizer. Inverse Fourier transformation is performed digitally on the measured temporal waveform to obtain the axial profile of the sample. Consequently, axial scanning is performed at the pulse repetition rate of 90.9 MHz. For tomographic image acquisition, an acousto-optic deflector is used for lateral scanning over the sample at 50 kHz.

#166938 - $15.00 USD Received 18 Apr 2012; revised 20 Jun 2012; accepted 22 Jun 2012; published 13 Aug 2012

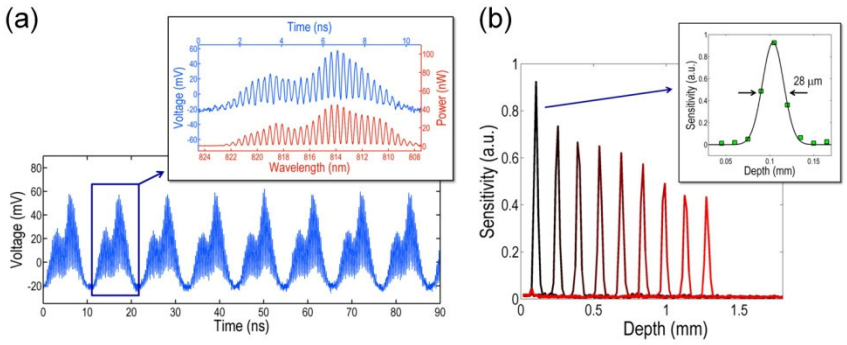

Fig. 2. Basic performance of time-stretch OCT. (a) Train of temporally dispersed pulses displayed on a high-speed oscilloscope. The interval between consecutive axial scans (pulses) is 11 ns, which corresponds to an axial scan rate of 90.9 MHz. The inset shows one-to-one mapping between the temporal waveform of one of the pulses measured by a real-time oscilloscope and the optical spectrum of the waveform measured by a conventional optical spectrum analyzer, validating photonic time-stretch in the 800 nm spectral range. (b) *Single-shot* point-spread functions at different imaging depths. The inset shows that the measured axial resolution is 28 μm and is in good agreement with the theoretical estimate of 21 μm.

2.2 Basic performance and theoretical analysis

The basic performance of the time-stretch OCT is shown in Fig. 2. The temporally dispersed pulse train displayed on a high-speed oscilloscope is shown in Fig. 2(a), the inset of which indicates one-to-one mapping between the temporal waveform and the spectrum of the waveform measured by a conventional optical spectrum analyzer. The *single-shot* point-spread functions at different imaging depths are shown in Fig. 2(b), the inset of which indicates the method's reasonable imaging capability with an axial resolution of 28 μm.

A theoretical analysis of the time-stretch OCT system was performed to evaluate its performance shown in Fig. 2. First, the axial range is estimated to be 1.3 mm, which we obtained from the relation $\Delta z = \lambda_0^2 / 4\delta\lambda$ [6–8], where $\lambda_0 =$ 815 nm is the center wavelength and $\delta\lambda$ is the spectral resolution of the photonic time stretcher. Here $\delta\lambda$ is given by $\delta\lambda = \delta t / D$ [6–8], where λt is the temporal resolution of the detection system and D is the total GVD of the dispersive fiber given by $D = -615$ ps/nm. The dispersive fiber we used has a linear GVD coefficient of −123 ps/nm/km over 20 nm centered about 815 nm, an absorption loss of 3.2 dB/km, and a length of 5 km. Second, the theoretical limit on the axial resolution is found to be 21 μm from the relation, $\delta z = \left(2\ln 2 / \pi\right)\left(\lambda_0^2 / \Delta\lambda\right)$ [6–8], where $\Delta\lambda =$ 14 nm is the optical bandwidth, and is in good agreement with the measured axial resolution (28 μm).

For designing a time-stretch OCT system, it is important to take the relations between these basic parameters (i.e., axial range, axial resolution, axial scan rate, GVD, and optical bandwidth) into account. Since consecutive temporally-stretched pulses cannot be overlapped with each other, given the pulse repetition rate (R), there is an upper limit on the optical bandwidth such that $\Delta t = D\Delta\lambda < 1/R$, where Δt is the width of the temporally-stretched pulse. This relation translates into a lower limit on the axial resolution such that $\delta z > \left(2\ln 2 / \pi\right)\left(DR\lambda_0^2\right)$. From the parameter values used in this experiment, the lower limit is found to be 17 μm. Alternatively, combining the equations, a trade-off relation between the axial range and resolution can also be obtained, such that $\Delta z / \delta z < \pi / \left[\left(8\ln 2\right)\left(R\delta t\right)\right]$.

The sensitivity of time-stretch OCT in this proof-of-principle demonstration was measured to be 42 dB (using a variable attenuator in the sample arm of the interferometer) and limited by the electronic noise of the photodetector and the quantization noise of the

#166938 - $15.00 USD Received 18 Apr 2012; revised 20 Jun 2012; accepted 22 Jun 2012; published 13 Aug 2012

digitizer which are typically large in high-speed detection. Here, the system sensitivity is theoretically estimated to be 45 dB from the optical power in each interferometer arm (0.5 mW), the digitizer's quantization noise in the window of 500 mVpp (12.8 nV/Hz$^{1/2}$), and the photodetector's quantum efficiency (0.6), noise-equivalent power (27 pW/Hz^{½}), and bandwidth (12 GHz). Note that the dominant noise source is the quantization noise of the digitizer which is very large due to the high-speed nature of the electronic circuitry. Details about the signal and noise of photonic time-stretch systems can be found in Ref [15]. The sensitivity can be improved significantly by employing optical pre-amplification before photodetection, a Mach-Zehnder interferometer in a balanced detection scheme [2–5], or a high-resolution digitizer with low quantization noise. Our analysis shows that the sensitivity of time-stretch OCT can be improved to 80 dB or higher. For instance, an optical amplification of 20 dB followed by a 12-bit digitizer may be used to achieve this goal.

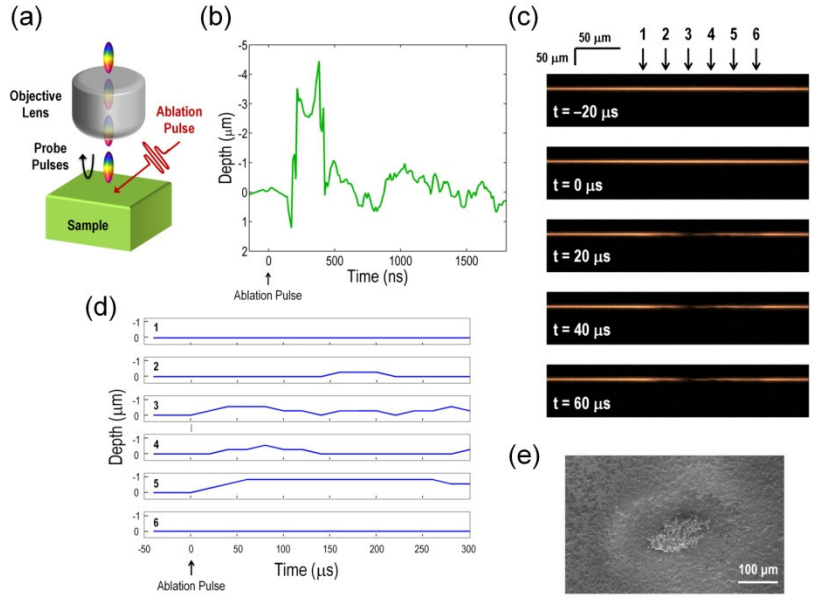

Fig. 3. Real-time observation of laser ablation dynamics with time-stretch OCT. (a) Schematic of the laser ablation experiment. The ablation was performed with a single 5 ns mid-infrared laser pulse focused at an angle onto the silicon sample. The 800 nm pulse train of time-stretch OCT was incident normal onto the surface through the objective lens for real-time monitoring of dynamic changes in the sample's surface axial position during the laser ablation. (b) Dynamics of the axial profile of the ablated surface at a single transverse point. The entire axial profile sequence corresponding to the dynamics (laser-induced mass ejection) caused by the single ablation pulse was captured at an axial scan period of 11 ns in real time. The figure indicates that the sample exploded at t = 200 ns after the ablation pulse arrived at the target at t = 0 ns. The finite time delay between the ablation pulse and the sudden depth change is due to the phase-explosion effect. The standard deviation of the fluctuations in the depth of the reference layer and the ablated layer before the explosion was measured to be 54 nm, which is small relative to the laser induced changes in the axial profile of the sample. (c) Sequence of successive tomographic images with a lateral scan period of 20 μs (corresponding to the lateral scan rate of 50 kHz). The ultrafast tomographic image acquisition was made possible by our ultrafast axial scanning. (d) Axial positions at different lateral points around the ablation region indicated in Fig. 3(c). (e) Scanning electron microscope image of the ablated sample, indicating the production of the crater by the laser ablation.

3. Utility of high-throughput OCT

To show the ultrafast axial profiling capability of time-stretch OCT, we performed real-time observation of laser ablation dynamics. Laser ablation - removal of material with short powerful laser pulses - is a ubiquitous technology used in laser surgery, material synthesis,

#166938 - $15.00 USD Received 18 Apr 2012; revised 20 Jun 2012; accepted 22 Jun 2012; published 13 Aug 2012

and laser cutting and micromachining and is an ideal testbed for time-stretch OCT. As shown in Fig. 3(a), the ablation was performed with a single mid-infrared laser pulse (with a fluence of 20 J/cm^2 and pulse width of 5 ns at a wavelength of 2.8 μm) focused at an angle onto a silicon sample. The 800 nm pulse train of the time-stretch OCT was incident normal onto the surface through an objective lens (NA = 0.4) for real-time monitoring of dynamic changes in axial profile during the laser ablation. The lateral resolution is 2 μm (in the lateral scan direction) and 1 μm (in the direction perpendicular to the lateral scan direction) while the lateral range is 260 μm.

The real-time axial profile of the ablated layer at a single lateral point (i.e., without lateral scanning) is shown in Fig. 3(b). The entire axial profile sequence corresponding to the laser ablation dynamics (laser-induced mass ejection) was captured with an axial scan period of 11 ns in real time. The figure indicates that the silicon surface exploded at t = 200 ns after the ablation pulse arrived at the target at t = 0 ns. The finite time delay between the arrival of the ablation pulse and the sudden depth change is due to the phase-explosion effect [16,17]. The standard deviation of the fluctuations in the axial position of the ablated surface before the explosion was measured to be 54 nm, which is small relative to the ablation-induced changes.

For tomographic image acquisition, we performed the same experiment with lateral scanning. As shown in Fig. 3(c), we obtained a sequence of successive tomographic images with a lateral scan period of 20 μs (corresponding to the lateral scan rate of 50 kHz). The ultrafast tomographic image acquisition was made possible by our ultrafast axial scanning. Figure 3(d) shows the dynamics of the sample surface at different lateral points indicated in Fig. 3(c). Since the major part of the explosion occurred within 1 μs after the arrival of the ablation pulse, the lateral scan period of 20 μs did not allow us to see it dynamically although the post-explosion dynamics of the sample is evident on the time scale of 100 μs. A scanning electron microscope image of the ablated sample is shown in Fig. 3(e), indicating the crater produced by the ablation process.

4. Summary

In summary, we have demonstrated a method for high-throughput OCT that offers ultrahigh axial scan rate in the 800 nm spectral range. This system is based on the use of photonic time-stretch with a single-mode fiber with a smaller effective mode area than conventional fibers in the wavelength operation range for increased contribution of waveguide dispersion to the total chromatic dispersion of the fiber. As a proof-of-principle demonstration, we have shown a record high axial scan rate of 90.9 MHz, and applied the OCT system to real-time observation of laser ablation dynamics. Since the sensitivity of time-stretch OCT is much lower than that of conventional OCT (which operates at low axial rates) due to the large bandwidth of the detection system, we expect that it is useful for non-biological applications (e.g., industrial applications) where high axial scan rates are required at the expense of reduced sensitivity, such as material characterization, microfluidics, and manufacturing and process control.

Acknowledgments

This work was partially supported by the Microsystems Technology Office (MTO) in the U.S. Defense Advanced Research Projects Agency (DARPA). We are grateful to K. Y. Hon and K. K. Tsia for valuable discussions and assistance with the experimental setup. K. Goda holds a Career Award at the Scientific Interface from the Burroughs Wellcome Fund.

#166938 - $15.00 USD Received 18 Apr 2012; revised 20 Jun 2012; accepted 22 Jun 2012; published 13 Aug 2012